Journal of the European Ceramic Society Volume 29, Issue 15, 1 December 2009, Pages 3273-3278

Investigation of the dielectric and piezoelectric properties of potassiumsodium niobate ceramics close to the phase boundary at $(K_{0.35}Na_{0.65})NbO_3$ and partial substitutions with lithium and antimony

Henry Ekene Mgbemere[a], Ralf-Peter Herber[b], Gerold A. Schneider[a],*

a *Institute of Advanced Ceramics, Hamburg University of Technology, Denickestrasse 15, 21073 Hamburg, Germany*
b *Department of Ceramics and Glass Engineering, CICECO, University of Aveiro, 3810-193 Aveiro, Portugal*

* Corresponding author.
E-mail addresses: henry.mgbemere@tu-harburg.de (H.E. Mgbemere), g.schneider@tu-harburg.de (G.A. Schneider).

Abstract
Potassium sodium niobate (KNN) piezoelectric ceramics and KNN substituted with lithium (Li^+) and antimony (Sb^{5+}) have been synthesized by the conventional solid state sintering method. This work focuses on the phase transition in the KNN system at potassium (K^+) content of approximately 0.35. Therefore, K amount was altered from 0.31 to 0.35. Additionally, Li^+ and Sb^{5+} were used for partial substitution (up to 8% for Sb) thereby enhancing the piezoelectric and dielectric properties. However, addition of Li+ and Sb5+ also lead to a decrease in both the Curie temperature (T_C) and the first order phase transition temperature ($T_{T\text{-}O}$) of the ceramics. Addition of more than 4 mol% of Li^+ led to the formation of extra phases. The piezoelectric properties within the given composition range were found to be optimum at $(K_{0.34}Na_{0.64}Li_{0.02})(Nb_{0.96}Sb_{0.04})O_3$. A piezoelectric charge coefficient (d_{33}) of 404 pm/V for this composition was obtained from unipolar strain hysteresis measurements.

1. Introduction
The high piezoelectric properties exhibited by lead zirconate titanate (PZT) based piezoelectric ceramics have been attributed to the morphotrophic phase boundary (MPB) phenomenon where two crystallographic phases are believed to coexist[1]. The environmental concerns about the harmful effects of lead however have necessitated using alternative piezoelectric ceramics in devices that were formerly produced using lead based ceramics. Among the many alternatives, potassium sodium niobate (KNN) based piezoelectric ceramics are considered to be possible replacements because of their relatively high Curie temperature (T_C), good ferroelectric properties and high electromechanical coupling coefficient especially

when produced by hot pressing.[2] This belief has been further reinforced since Saito et al.[3] reported on improved piezoelectric properties of KNN by element substitution and texturing. In the KNN system, there are three phase boundaries where the properties appear to be optimum. These phase boundaries correspond approximately to x = 0.17, 0.35 and 0.5 respectively.[1] Earlier publications on KNN made mention of these transitions, for instance Shirane et al.[4] studied the dielectric properties and phase transitions in (K,Na)NbO_3 crystals in order to show the relationship between the various phases of the solid solution.

Ahtee and Glazer[5] determined the lattice parameters and nature of the tilted octahedron in $(Na_{1-x}K_x)NbO_3$ solid solutions. Ahtee et al. used neutron diffraction to give a more detailed picture of what is happening during the structural phase transitions by determining the magnitudes and directions of atomic displacements. Recently the research focus has been to improve both the sinterability and piezoelectric properties of KNN by investigating solid solutions such as KNN-$CaTiO_3$,[7] KNN-$SrTiO_3$,[7,8] KNN-BaO,[9] KNN-$LiNbO_3$,[10] KNN-$LiTaO_3$,[11] KNN-$LiTaO_3$-$LiSbO_3$,[3] and KNN-$LiSbO_3$.[12] It is commonly accepted that the piezoelectric properties appear to be optimum when the amount of K^+ on the A-site of the perovskite is approximately equal to 0.5 mol.[2] As a result, most of the reports have concentrated on this phase boundary with little information in the literature with respect to the properties of the other phase boundaries in both the undoped and doped form.

The objective of this paper is to investigate the phase boundary in the KNN system with K^+ content of approximately 0.35 mol. At this composition, two monoclinic phases of the same Space group (P1M1) are separated by the phase boundary. The crystal structure of the phase with higher K^+ content (a = 7.9751(7) Å, b = 7.8620(4) Å, c = 7.9565(6) Å, β = 90.34(0)°) has oxygen octahedra that are slightly tilted about the b-axis of the unit cell whereas at lower K^+ contents (a = 7.9162(9) Å, b = 7.835(4) Å, c = 7.8993(9) Å, β = 90.32(0)°) a tilting about the a and b-axis with opposite orientations is observed.[6] As is evident in the β values, the two structures are close to the orthorhombic structure and will therefore further on be addressed as such, to facilitate comparison with the orthorhombic and tetragonal phases at $(K_{0.5}Na_{0.5})NbO_3$. Furthermore, we will compare the properties of the material in the undoped form and when both the A and B-sites of the perovskite structure are substituted with different amounts of Li and Sb respectively.

2. Experimental procedure

$(K_xNa_{1-x})NbO_3$ (x = 0.31, 0.32, 0.33, 0.34, 0.35) abbreviated KNN and $(K_{0.35-1/2y}Na_{0.65-1/2y})Li_y(Nb_{1-2y}Sb_{2y})O_3$ (y=0, 0.02, 0.04, 0.06, 0.08) abbreviated as KNN–LS were synthesized through the mixed oxide route with the following powders: K_2CO_3, Na_2CO_3, Li_2CO_3 (99%), Nb_2O_5 and Sb_2O_3 (99.9%) (Chempur Feinchemikalien und Forschungs GmbH, Karlsruhe, Germany). The powders were first weighed and dried separately at 200°C for 4 h. They were then mixed and attrition milled for 4 h using ethanol as solvent and zirconia balls as the millingmedia. Calcination was carried out at 800°C for 4 h in air. Another attrition milling and calcination processwas carried out to ensure that there was homogeneity in the powder composition and to continue the process of phase formation.

The powders were then pressed into discs of approximately 12.5mm diameter and 4.5mm thickness initially using a 170MPa uniaxial pressure and subsequently a cold isostatic press at 500MPa for 2 min. The KNN pellets were sintered at 1080°C, 1100°C while the KNN–LS pellets were at 1060°C, 1080°C, 1100°C and 1120°C for 1 h in air atmosphere respectively. Densities of the samples were determined using the Archimedes method and the samples were subsequently ground and polished for characterisation. The crystal structures of the sintered samples were examined using X-ray diffraction (XRD) analysis with Cu K_ radiation (λ = 1.54178 Å) (D8 Discover, Bruker AXS, Karlsruhe, Germany) while the whole powder pattern decomposition was done with Pawley fitting method in Topas. Silver paints acting as electrodes were applied on both surfaces of the samples for dielectric and piezoelectric property measurements. The samples were poled using 2 kV/mm in silicon oil bath at 80°C for 10 min. The temperature dependence of the dielectric properties of the ceramics was measured from 20 Hz to 1MHz with an LCR meter (HP 4284A, Agilent Technologies, Inc., Palo Alto, USA) attached to a heating chamber. The polarisation hysteresis measurements were carried out using the standard Sawyer–Tower circuit while the strain hysteresis was measured with an inductive transducer device (HBM, Hottinger Baldwin Messtechnik,Darmstadt, Germany). A complete dipolar hysteresis measurement was performed in 200 s. The piezoelectric coefficient d_{33} was measured using a low signal displacement transducer connected to a lock-in amplifier as well as with high signal unipolar strain hysteresis measurements.

3. Results

Fig. 1 shows the bulk density values for KNN–LS samples as a function of sintering temperature. The values for y = 0, 0.02 and 0.04 for temperatures up to 1100°C varied between 4.1 g/cm^3 and 4.3 g/cm^3. Above 1100°C, there is a decrease in the density value for all the samples. This is possibly because the vapour pressure of elements like K^+ and Li^+ increased and led to a decrease in weight of the samples. The density values for y = 0.06 and 0.08 increased with increasing sintering temperature up to 1100°C. The increase in the density value (~10%) compared with the other samples sintered between 1080°C and 1120°C can be attributed to the formation of extra phases as shown in the XRD data in Fig. 3. For KNN samples with compositions x = 0.31–0.35, the density values obtained are as shown in Table 1. The obtained values generally showed only small differences and range from 4.2 g/cm^3 to 4.3 g/cm^3 which corresponds to between 93.3% and 95.5% of their theoretical densities. The XRD patterns for KNN and KNN–LS samples are as shown in Figs. 2 and 3 respectively. All the characterizations except for density determination were carried out using the samples sintered at 1080°C. All the KNN samples show a single phase however a higher resolution powder diffractometer may be required to spot differences (if there are any) in the patterns. For the KNN–LS samples, single phases were formed when $y \leq 0.04$ while extra phases were formed with higher concentrations. The distortion in the patterns decreased with increasing amount of the substituents. From the International Centre for Diffraction Data (ICDD) database, the possible patterns that tend to match these extra phases are the tetragonal tungsten bronze structures ($K_3Li_2Nb_5O_{15}$ and related structures).

PDF 01-077-0038 from ICDD, which is based on the paper by Ahtee et al. was used as a reference and has a monoclinic symmetry. The pattern is defined as$K_{0.65}Na_{0.35}NbO_3$ but a careful reading of the original article from which the reference was produced shows that the phase composition discussed is in fact $K_{0.35}Na_{0.65}NbO_3$. The search and match analysis that was carried out using our measured pattern gives a good matching with the reference material as shown in Fig. 4. Based on the composition $K_{0.65}Na_{0.35}NbO_3$ a theoretical density of 4.64 g/cm^3 was obtained for the reference, but with $K_{0.35}Na_{0.65}NbO_3$ we calculated the theoretical density to be 4.508 g/cm^3. The theoretical density values were created from the diffraction patterns and their respective percentages for samples sintered at 1080°C and 1100°C respectively are shown in Table 1. The temperature dependence of the dielectric constant for

the KNN sample is as shown in Fig. 5. The dielectric constant values for x = 0.35 is higher than that for x = 0.5 from the literature.[13–15] The first order phase transition for the measured samples occurred at approximately 202°C while there was a slight change in the T_C. The T_C for x = 0.35 is 412°C while it is ~405°C for both x = 0.33 and 0.3. For $K_{0.5}Na_{0.5}NbO_3$, the phase transition temperature found in the literature varies with different researchers with some reporting slightly higher[16,17] or lower[15,17,18] temperatures. The dielectric constant values at both the $T_{T\text{-}O}$ and T_C phase transitions are highest at x = 0.35 and lowest at x = 0.33. The values here are much higher than that reported for x = 0.5.[2,15,19] The temperature dependence of the dielectric loss for KNN is shown in Fig. 6. For x = 0.35, tan δ values remained stable (~3%) with temperature up to 450°C. This compares favourably with the values for x = 0.5 in the literature.[2,13,15,20] For the others, the tan δ increased slightly with increasing temperature and above 320°C, the dielectric loss increased substantially. Fig. 7 shows the dielectric constant values for KNN–LS samples at 100 KHz. Samples with composition y = 0, 0.02 and 0.04 have T_C of 412°C, 361°C and 328°C while their $T_{T\text{-}O}$ occurred at approximately 202°C, 131°C and 110°C respectively. This indicates that increasing the amount of Li and Sb in KNN decreases the temperature of both phase transitions. Increasing the substituents also lead to peak broadening at the T_C which is an indication that the sample behaves like a relaxor ferroelectric. The dielectric loss in the samples at 100 KHz is as shown in Fig. 8. At temperatures below 250°C, the loss factor was below 5% and above this temperature, the loss factor in the Li and Sb substituted samples increased almost exponentially and increases with increasing amount of substituents. The effect of lithium on the dielectric loss of KNN has been reported in the literature.[21] The increase in the loss factor with increasing temperature is attributed to the small ionic size of Li when compared to that of K and Na and consequently its ability to diffuse easily through the crystal lattice. The polarisation hysteresis loops for the KNN samples at room temperature as a function of the applied electric field is as shown in Fig. 9. All the samples showed saturation polarization (P_s) when an electric field of 20 kV/cm is applied. The sample with composition x = 0.35 has the highest remnant polarization (P_r) of 24 μC/cm^2 and also the lowest coercive field (E_c) of 8.7 kV/cm. This suggests that compared with the other samples, it has “soft” ferroelectric properties. The values for the other samples are as shown in Table 1. This value of P_r is higher than the values for the well-reported $K_{0.5}Na_{0.5}NbO_3$ ceramic but with lower E_C.[22–24] Fig. 10 shows the polarization hysteresis loops for the KNN–LS samples. The sample with y = 0.02 reached P_s with a P_r of 22.5 μC/cm^2. For y = 0.04, Ps could not be reached with the applied field. It was slightly conductive and so

the leakage cur-rent or space charges also contributed to the size of the hysteresis loop thereby making the P_r to be higher than P_s. For samples with $y > 0.04$, hysteresis loops could no be obtained because of very high leakage current which led to dielectric breakdown. The graph of strain as a function of electric field for sample composition $y = 0.02$ measured in the positive direction is as shown in Fig. 11. A piezoelectric charge coefficient of 378 pm/V was obtained after poling the sample with 1 kV/mm while 404 pm/V was obtained from 2 kV/mm. This is the highest value obtained using this measurement technique for all the samples. The d^*_{33} values for the other compositions are shown in Table 1. The KNN samples also gave relatively high values with $x = 0.34$ giving the highest d^*_{33} value.

4. Conclusion

Samples with composition $(K_xNa_{1-x})NbO_3$ and $(K_{0.35-1/2y}Na_{0.65-1/2y})Li_y(Nb_{1-2y}Sb_{2y})O_3$ were successfully synthesized using the conventional synthesis method for processing ceramics.

The theoretical densities for the ceramics were successfully calculated using the Pawley fitting method in Topas. The apparent density values for the samples were also calculated and for both compositions, density values between 90% and 96% were obtained. The diffraction patterns for KNN showed single perovskite phases while for KNN–LS, above $y = 0.04$, an extra phase had formed, which was attributed to a tetragonal tungsten bronze structure. We were also able to show that PDF 01-077-0038 from ICDD is in fact $K_{0.35}Na_{0.65}NbO_3$. The $T_{T\text{-}O}$ phase transition for the KNN samples occurred at approximately 202°C while the T_C for $x = 0.35$ occurred at 412°C and approximately 405°C for both $x = 0.33$ and 0.31 respectively which is close to the phase transition points at $x = 0.5$. Using Li and Sb to substitute elements in KNN led to a reduction in both phase transitions temperatures while the dielectric loss in all the samples were very low and stable at temperatures below 250°C. Good polarisation hysteresis loops with high P_r were obtained for the KNN samples while KNN–LS samples also showed high Pr values. The conductivity in the KNN–LS samples increased with increasing amount of the substituents causing high leakage currents in compositions with $y > 0.04$. From the unipolar strain hysteresis measurements, high d^*_{33} values were obtained especially for the composition where $y = 0.02$.

References

1. Jaffe, B., Jaffe, H. and Cook, W. R., *Piezoelectric Ceramics*. Academic Press, London, 1971.

2. Jaeger, R. E. and Egerton, L., Hot pressing of potassium–sodium niobates. *J. Am. Ceram. Soc.*, 1962, **45**, 209–213.

3. Saito, Y., Takao, H., Tani, T., Nonoyama, T., Takatori, K., Homma, T., Nagaya, T. and Nakamura, M., Lead-free piezoceramics. *Lett. Nat.*, 2004.

4. Shirane, G., Newnham, R. and Pepinsky, R., Dielectric properties and phase transitions of NaNbO3 and (Na,K)NbO3. *Phys. Rev. B*, 1954, **96**(3), 581–588.

5. Ahtee, M. and Glazer, A. M., Lattice parameters and tilted octahedra in sodium–potassium niobate solid solutions. *Acta Cryst.*, 1976, **434**, A32.

6. Ahtee, M. and Hewat, A. W., Structural Phase transitions in sodium–potassium niobate solid solutions by neutron powder diffraction. *Acta Cryst.*, 1978, **A34**, 309–317.

7. Park, H.-Y., Cho, K.-H., Paik, D.-S., Nahm, S., Lee, H.-G. and Kim, D.-H., Microstructure and piezoelectric properties of lead-free $(1-x)(Na_{0.5}K_{0.5})NbO_3$–$xCaTiO_3$. *J. Appl. Phys.*, 2007, **124101**, 102.

8. Bobnar, V., Mali, B., Holc, J., Kosec, M. and Steinhausen, R. H. B., Electrostrictive effect in lead-free relaxor $K_{0.5}Na_{0.5}NbO_3$–$SrTiO_3$ ceramic system. *J. Appl. Phys.*, 2005, 98.

9. Ahn, Z. S. and Schulze, W. A., Conventionally sintered $(Na_{0.5}K_{0.5})NbO_3$ with barium additions. *J. Am. Ceram. Soc.*, 1987, **70**, 18–21.

10. Song, H.-C., Cho, K.-H., Park, H.-Y., Ahn, C.-W., Nahm, S., Uchino, K. and Park, S.-H., Microstructure and piezoelectric properties of $(1-x)(Na_{0.5}K_{0.5})NbO_3$–$xLiNbO_3$ ceramics. *J. Am. Ceram. Soc.*, 2007, **90**(6), 1812–1816.

11. Saito, Y. and Takao, H., High performance lead-free piezoelectric ceramics in the (K,Na)NbO_3–$LiTaO_3$ solid solution system. *Taylor & Francis Group*, 2006, **338**, 17–32.

12. Wu, J., Xiao, D., Wang, Y., Zhu, J., Yu, P. and Jiang, Y., Compositional dependence of phase structure and electrical properties in $(K_{0.42}Na_{0.58})NbO_3$–$LiSbO_3$ lead-free ceramics. *J. Appl. Phys.*, 2007, **114113**, 102.

13. Birol, H., Damjanovic, D. and Setter, N., Preparation and characterization of $KNbO_3$ ceramics. *J. Am. Ceram. Soc.*, 2005, **88**, 1754–1759.

14. Egerton, L. and Dillion, D. M., Piezoelectric and dielectric properties of ceramics in the system potassium–sodium niobate. *J. Am. Ceram. Soc.*, 1959, **42**, 438–442.

15. Ringgaard, E. and Wurlitzer, T., Lead-free piezoceramics based on alkali niobates. *J. Eur. Ceram. Soc.*, 2005, **25**, 2701–2706.
16. Priya, S., Uchino, K. and Ando, A., Nonlead perovskite piezoelectric materials. *Ceramic Trans.-Development in dielectric materials and electronic devices*, 2005, 223–233.
17. Lin, D., Guo, M. S., Lam, K. H., Kwok, K.W. and Chan, H. L.W., Lead-free piezoelectric ceramic $(K_{0.5}Na_{0.5})NbO_3$ with MnO_2 and $K_{5.4}Cu_{1.3}Ta_{10}O_{29}$ doping for piezoelectric transformer application. *Smart Mater. Struct.*, 2008, **035002**, 17.
18. Matsubara, M., Yamaguchi, T., Kikuta, K. and Shin-Ichi, H., Synthesis and characterization of $(K_{0.5}Na_{0.5})(Nb_{0.7}Ta_{0.3})O_3$ piezoelectric ceramics sintered with sintering aid $K_{5.4}Cu_{1.3}Ta_{10}O_{29}$. *Jpn. J. Appl. Phys.*, 2005, **44**, 6618–6623.
19. Yang, Z., Chang, Y., Liu, B. and Wei, L., Effects of composition on phase structure, microstructure and electrical properties of $(K_{0.5}Na_{0.5})NbO_3$–$LiSbO_3$ ceramics. *Mater. Sci. Eng. A*, 2006, **432**, 292–298.
20. Lin, D., Kwok kw and Chan, Hlw., Phase transition and electrical properties of $(K_{0.5}Na_{0.5})(Nb_{1-x}Ta_x)O_3$ lead-free piezoelectric ceramics. *Appl. Phys. A*, 2008, **91**, 167–171.
21. Hagh, N. M., Jadidian, B. and Safari, A., Property-processing relationship in lead-free (K, Na, Li) NbO_3-solid solution system. *J. Electroceram.*, 2007, **18**, 339–346.
22. Zuo, R., Roedel, J., Chen, R. and Li, L., Sintering and electrical properties of lead-free $Na_{0.5}K_{0.5}NbO_3$ piezoelectric ceramics. *J. Am. Ceram. Soc.*, 2006, **89**(6), 2010–2015.
23. Shimojo, Y., Wang, R., Sekiya, T. and Matsuzaki, K., Dielectric and piezoelectric properties of MeTiO3 (Me =Ba and Sr) modified (K,Na)NbO_3. *J. Korean Phys. Soc.*, 2005, **46**(1), 48–51.
24. Wang, R., Xie, R., Sekiya, T., Shimojo, Y., Akimune, Y., Hirosaki, N. and Mitsuru, I., Piezoelectric properties of spark-plasma-sintered $(Na_{0.5}K_{0.5})NbO_3$–$PbTiO_3$ ceramics. *Jpn. J. Appl. Phys.*, 2002, **41**, 7119–7122.

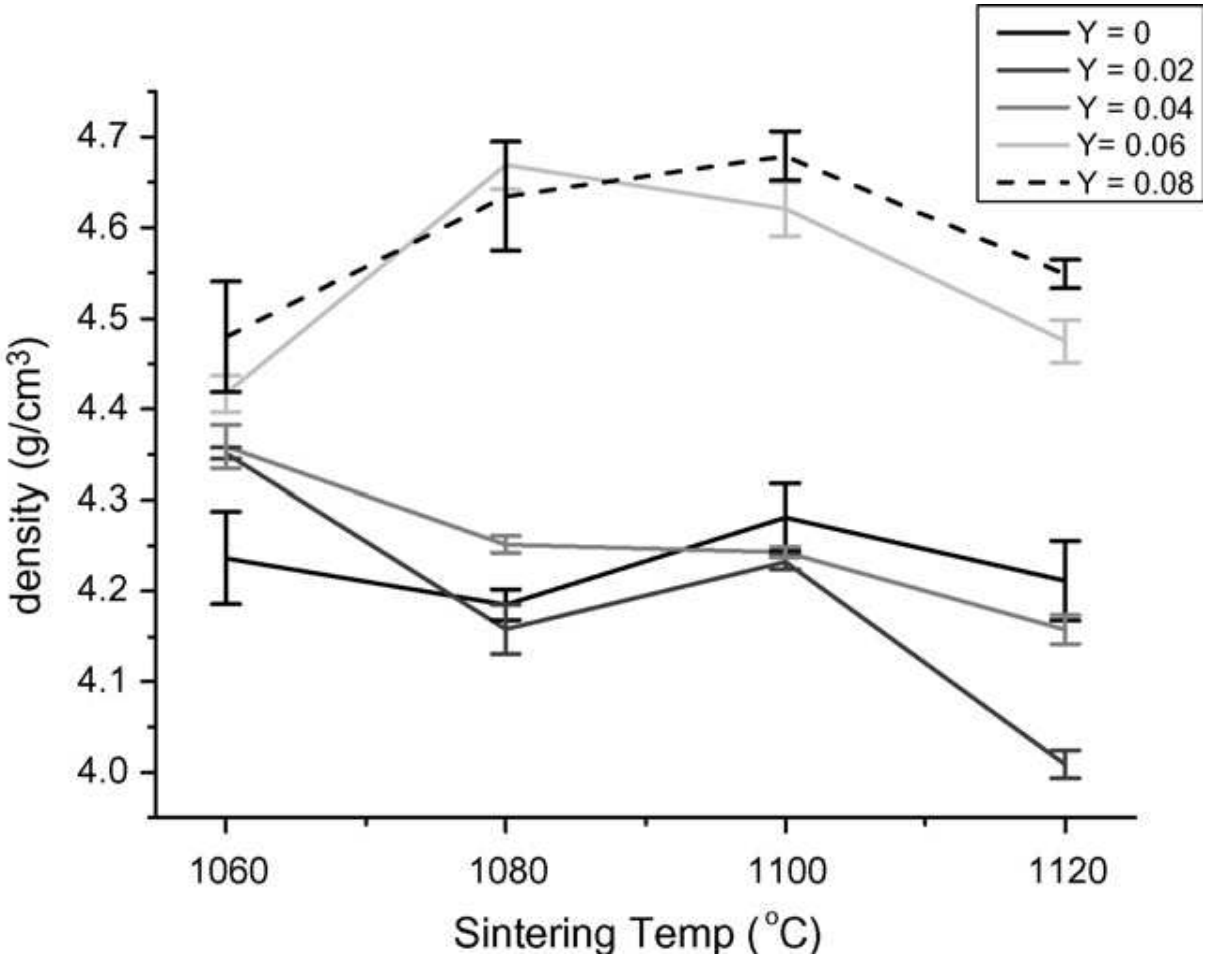

Fig. 1. Graph of density for KNN–LS ceramics with standard deviation as a function of sintering temperature.

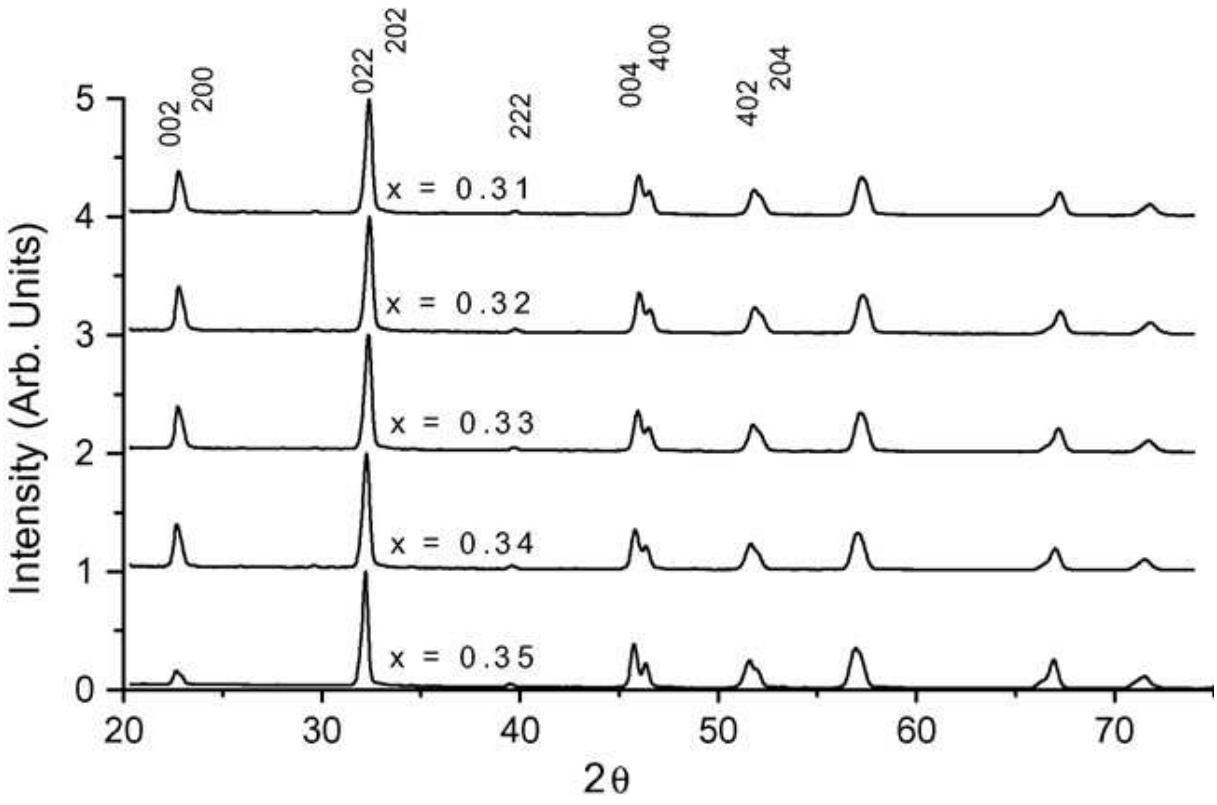

Fig. 2. XRD patterns of $K_xNa_{1-x}NbO_3$ samples where x ranges from 0.31 to 0.35 showing 2θ values from 20° to 75° and arbitrary intensity values. The samples were sintered at 1080°C for 1 h.

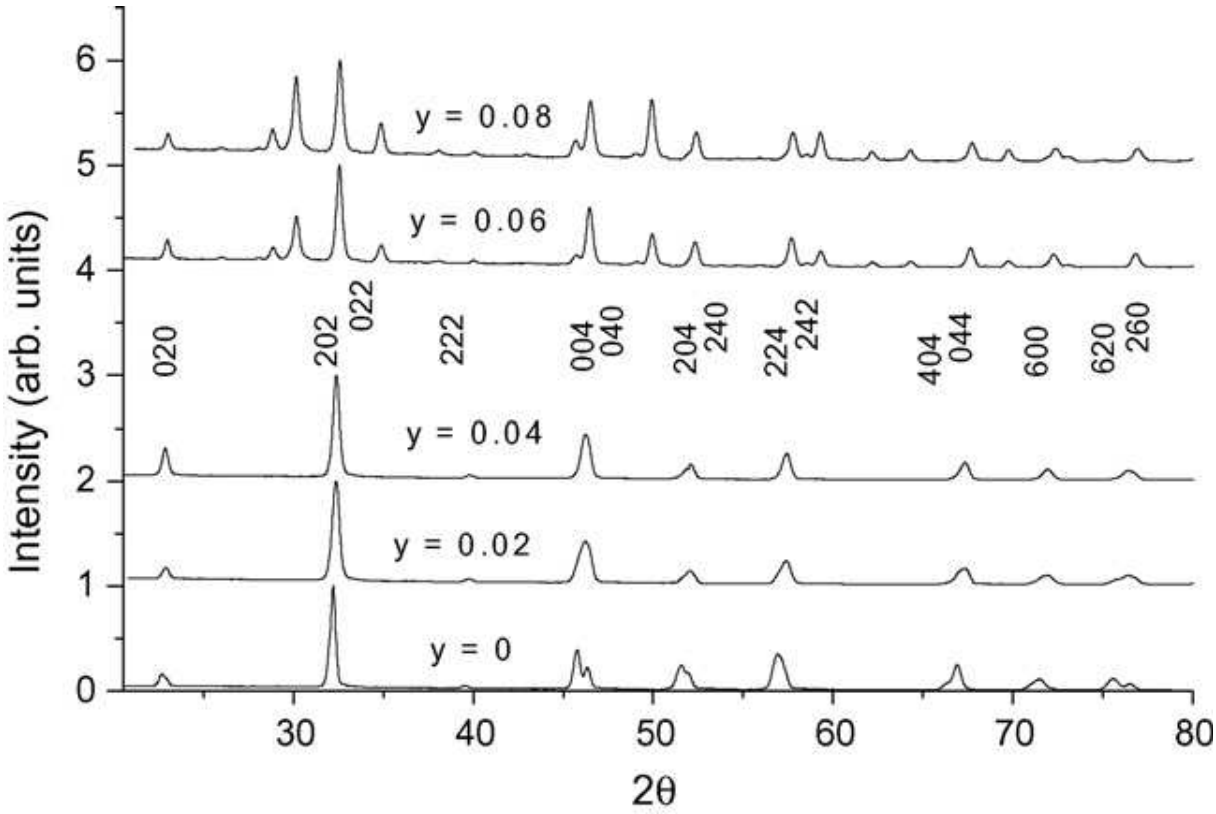

Fig. 3. XRD patterns of KNN–LS samples where y ranges from 0 to 0.08 showing 2θ values from 20◦ to 80◦ and arbitrary intensity values. The samples were sintered at 1080°C for 1 h.

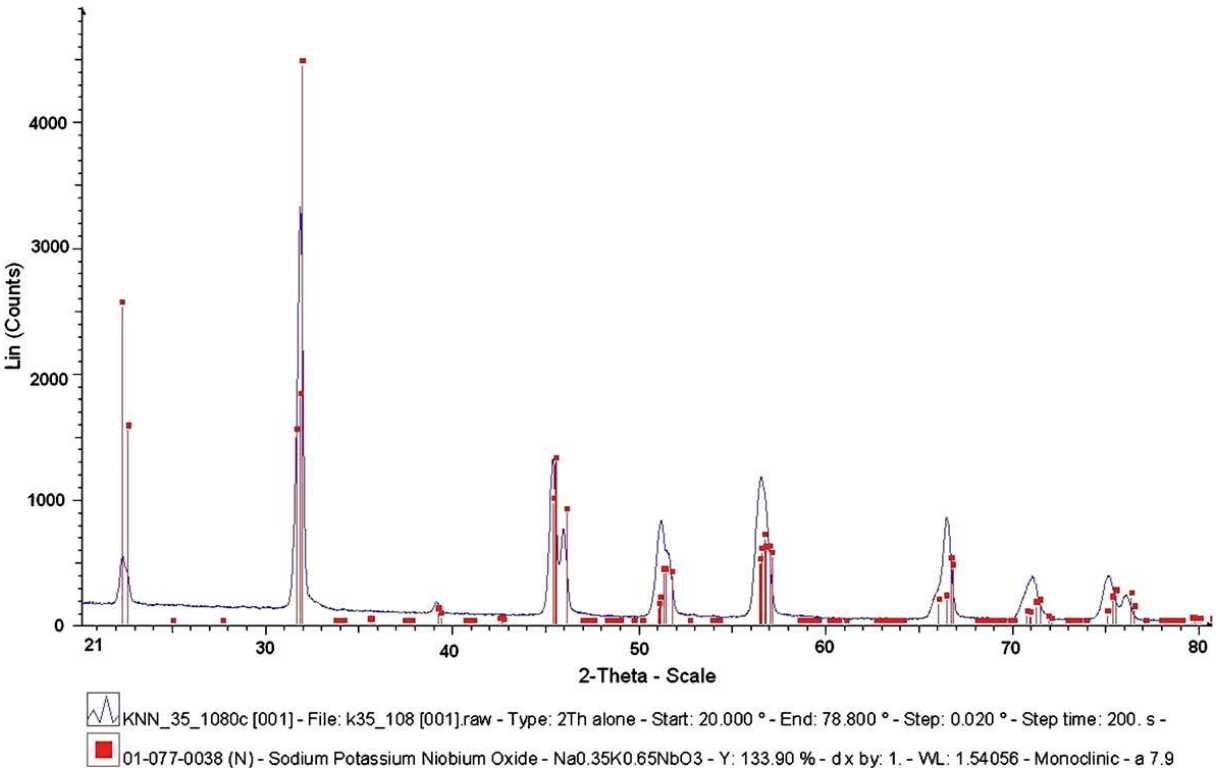

Fig. 4. XRD pattern of K0.35Na0.65NbO3 fitted with reference plot (PDF 01-077-0038) from ICDD.

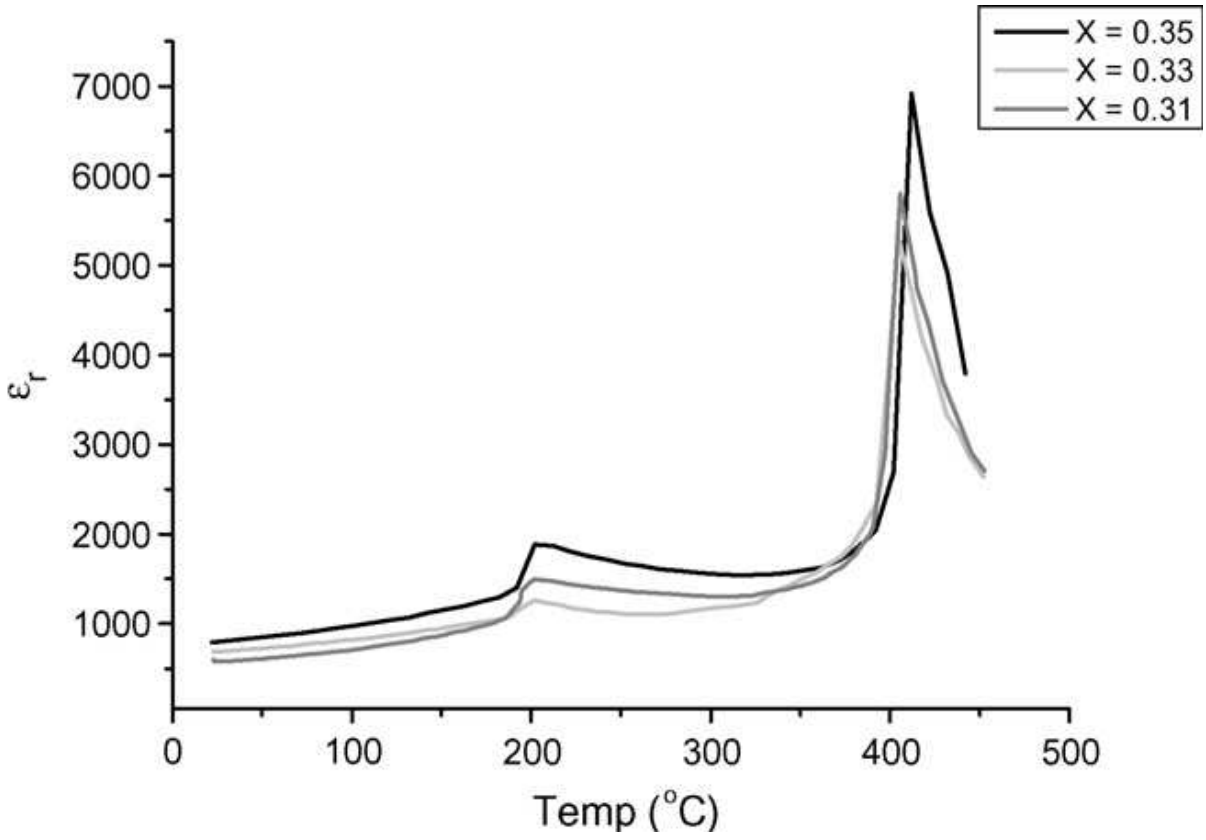

Fig. 5. Temperature dependence of dielectric constant for KNN samples(x = 0.35, 0.33 and 0.31) at 100 KHz.

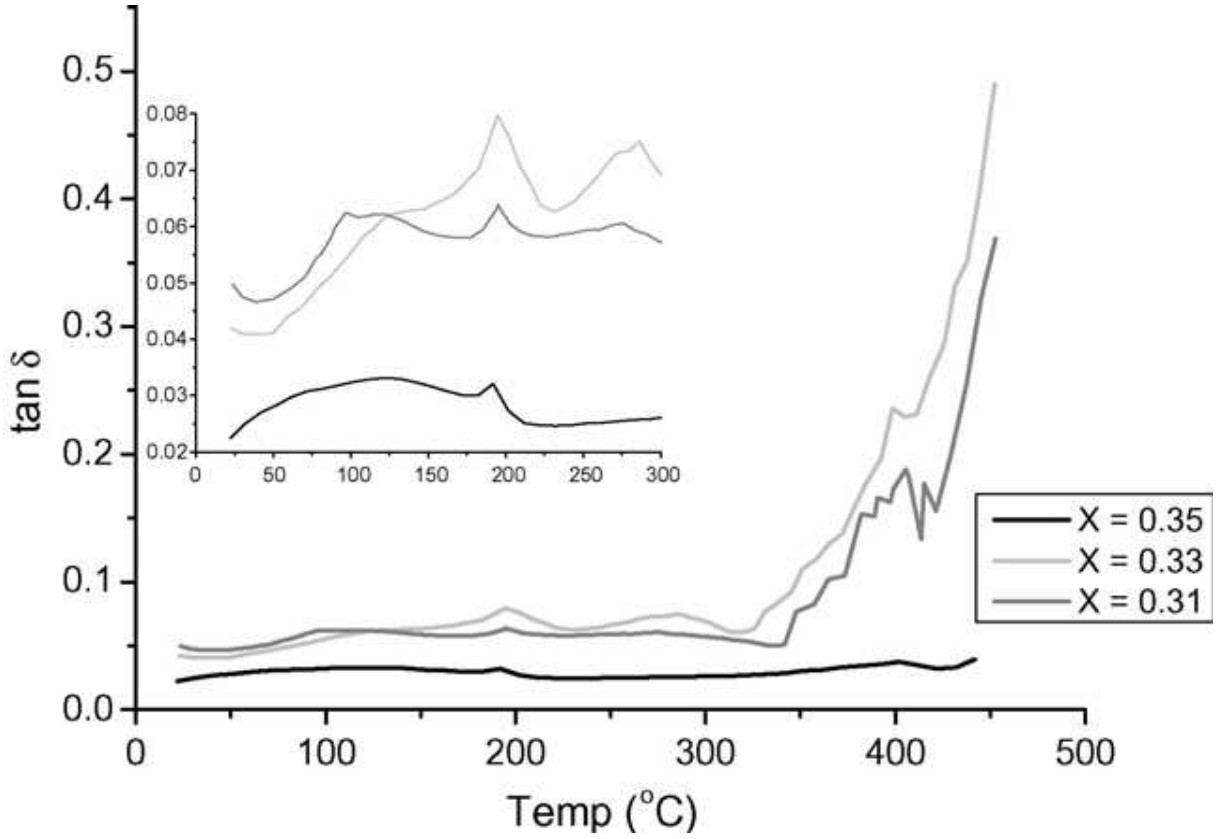

Fig. 6. Temperature dependence of dielectric loss for KNN samples (x = 0.35, 0.33 and 0.31) at 100 KHz.

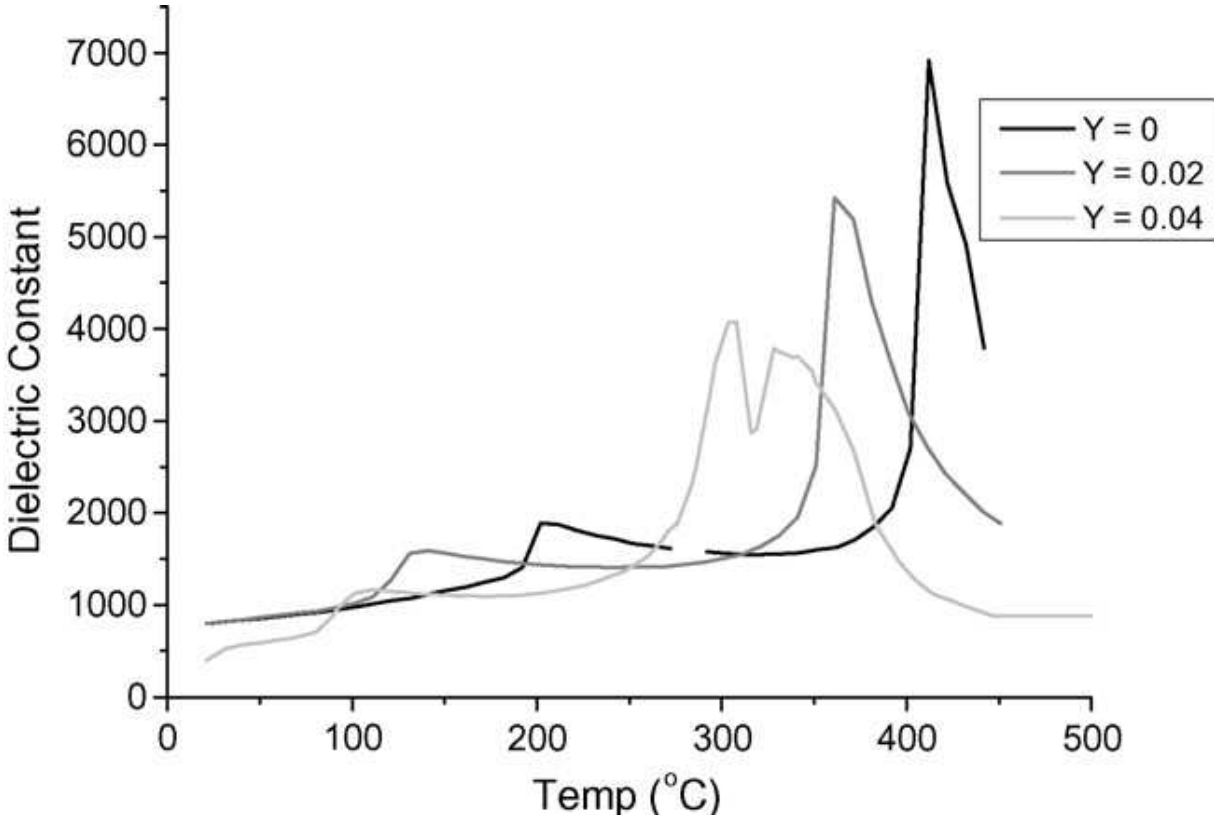

Fig. 7. Temperature dependence of dielectric constant for KNN–LS samples (y = 0, 0.02 and 0.04) at 100 KHz.

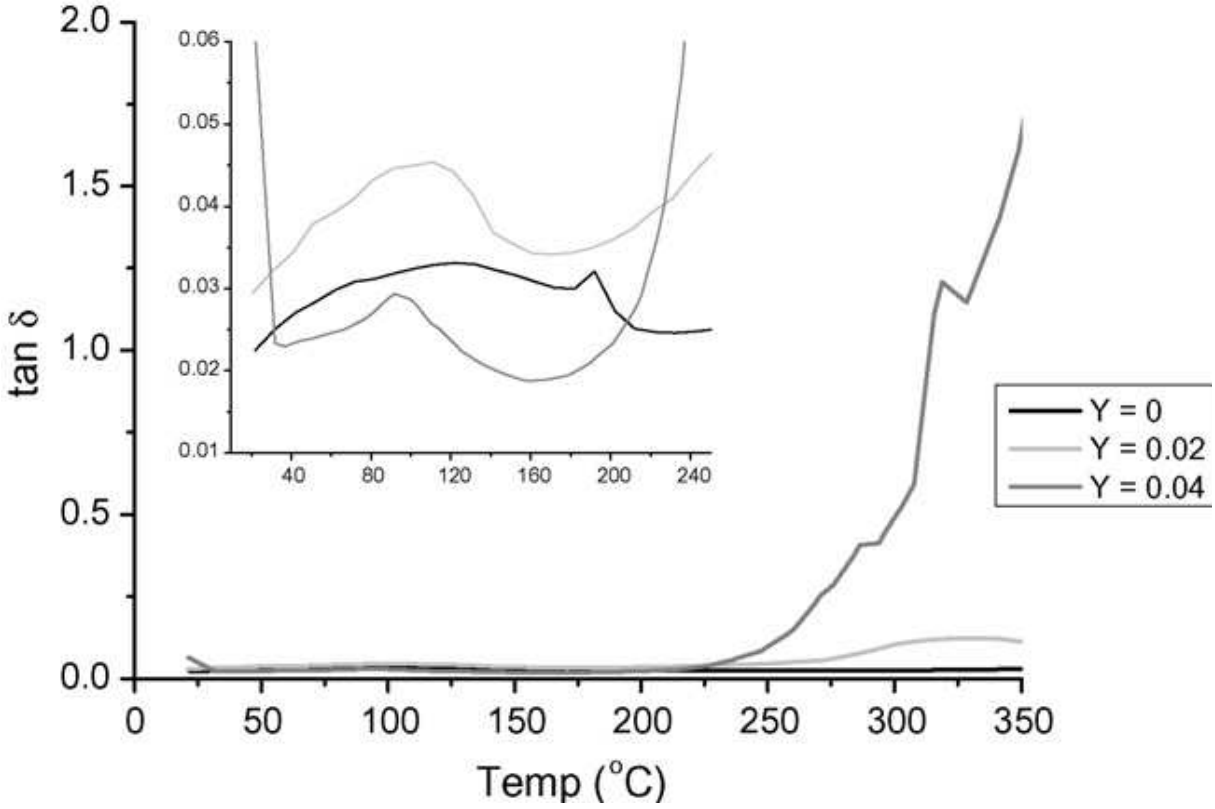

Fig. 8. Temperature dependence of dielectric constant for samples (x = 0.35, 0.33 and 0.31) at 100 KHz.

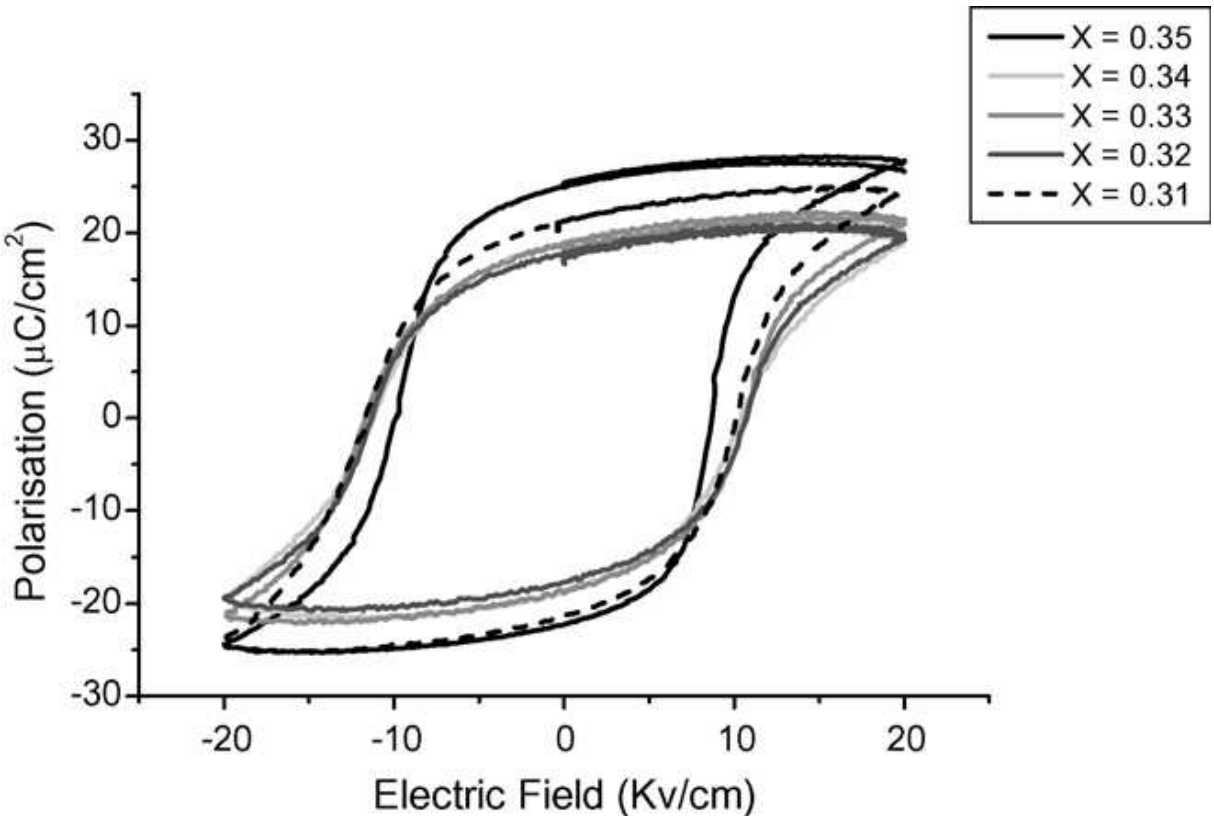

Fig. 9. Variation of P-E hysteresis loops for $K_xNa_{1-x}NbO_3$ ceramics.

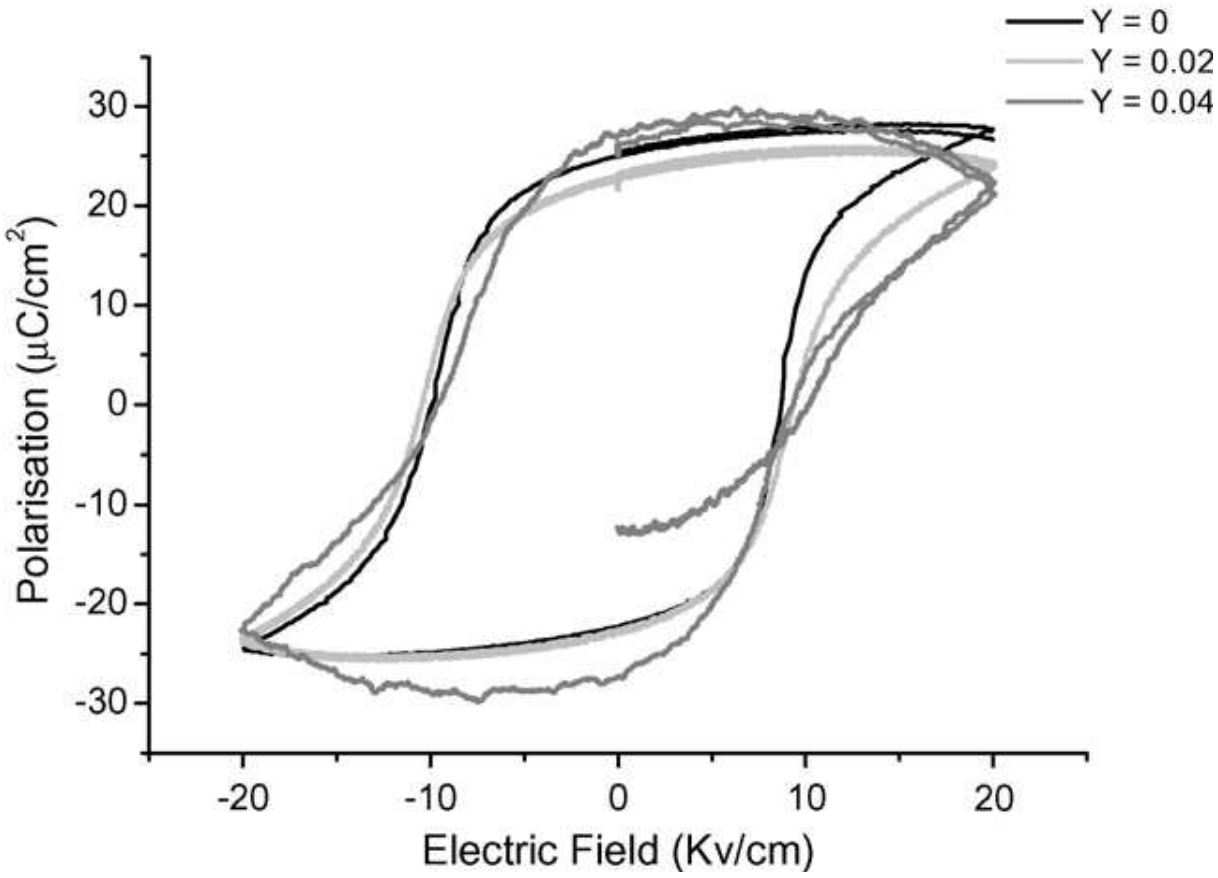

Fig. 10. Variation of P-E hysteresis loops for KNN–LS ceramics.

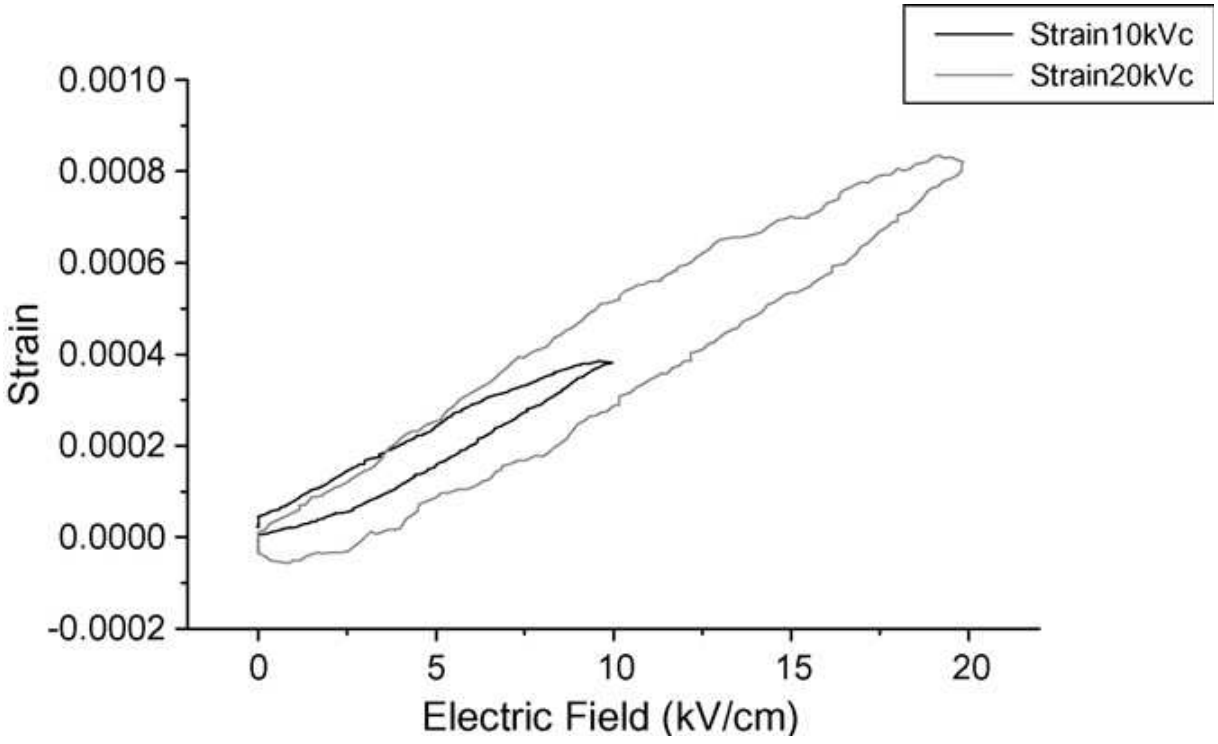

Fig. 11. Unipolar strain hysteresis measurement for $(K_{0.34}Na_{0.64}Li_{0.02})(Nb_{0.96}Sb_{0.04})O_3$ ceramic.

Table 1. Table showing the density values, dielectric and piezoelectric properties of KNN and KNN–LS ferroelectric ceramics.

Composition	x=0.35	x= 0.34	x=0.33	x=0.32	x=0.31	y=0.02	y=0.04
Theoretical ρ [g/cm3]	4.508	4.504	4.501	4.50	4.49	4.55	4.58
ρ % @ 1080℃	92.8±0.37	93.2±0.67	94.1±1.45	92.4±0.62	95.9±0.64	91.4±0.6	92.65±0.2
ρ % @ 1100℃	95±0.8	94.9±0.45	93.5±0.75	95.4±0.56	95.4±0.68	93±0.18	90.8±0.12
$_C$ [kV/mm]	8.7	10.5	10.5	10.5	10	10	9.5
P_r [μC/cm^2]	24	19.1	19.1	17.6	21.3	22.5	27
ε_r @T_C100kHz	6868	-	5311	-	5800	5800	4093
tan δ@100kHz	0.025	-	0.066	-	0.059	0.046	0.097
d_{33}* [pm/V]	125	167	156	123	163	404	205

d_{33}* here the piezoelectric charge coefficient was obtained from the slope of high voltage unipolar strain hysteresis measurement (20 kV/cm).